



Published in final edited form as:

Epilepsia. 2012 June ; 53(6): 1024–1032. doi:10.1111/j.1528-1167.2012.03466.x.

Abnormal structural and functional brain connectivity in gray matter heterotopia

Joanna A. Christodoulou, Ed.D.¹, Linsey M. Walker, B.A.², Stephanie N. Del Tufo, B.A.¹, Tami Katzir, Ph.D.³, John D. E. Gabrieli, Ph.D.¹, Susan Whitfield-Gabrieli, Ph.D.¹, and Bernard S. Chang, M.D.²

¹Department of Brain and Cognitive Sciences, Massachusetts Institute of Technology, Cambridge, MA

²Comprehensive Epilepsy Center, Department of Neurology, Beth Israel Deaconess Medical Center and Harvard Medical School, Boston, MA

³Department of Learning Disabilities, University of Haifa, Haifa, Israel

Summary

Purpose—Periventricular nodular heterotopia (PNH) is a malformation of cortical development associated with epilepsy and dyslexia. Evidence suggests that heterotopic gray matter can be functional in brain malformations and that connectivity abnormalities may be important in these disorders. We hypothesized that nodular heterotopia develop abnormal connections and systematically investigated the structural and functional connectivity of heterotopia in patients with PNH.

Methods—Eleven subjects were studied using diffusion tensor tractography and resting-state functional connectivity MRI with bold oxygenation level-dependent (BOLD) imaging. Fiber tracks with a terminus within heterotopic nodules were visualized to determine structural connectivity, and brain regions demonstrating resting-state functional correlations to heterotopic nodules were analyzed. Relationships between these connectivity results and measures of clinical epilepsy and cognitive disability were examined.

Key Findings—A majority of heterotopia (69%) showed structural connectivity to discrete regions of overlying cortex, and almost all (96%) showed functional connectivity to these regions (mean peak correlation coefficient 0.61). Heterotopia also demonstrated connectivity to regions of contralateral cortex, other heterotopic nodules, ipsilateral but nonoverlying cortex, and deep gray matter structures or the cerebellum. Subjects with the longest durations of epilepsy had a higher degree of abnormal functional connectivity ($p=0.036$).

Significance—Most heterotopic nodules in PNH are structurally and functionally connected to overlying cortex, and the strength of abnormal connectivity is higher among those with the longest durations of epilepsy. Along with prior evidence that cortico-cortical tract defects underlie dyslexia in this disorder, the current findings suggest that altered connectivity is likely a critical substrate for neurological dysfunction in brain malformations.

Corresponding author: Bernard S. Chang, M.D., Comprehensive Epilepsy Center, E/KS-457, Beth Israel Deaconess Medical Center, 330 Brookline Ave, Boston, MA 02215, phone 617-667-2889; fax 617-667-7919, bchang@bidmc.harvard.edu.

Disclosures

None of the authors has any conflict of interest to disclose. We confirm that we have read the Journal's position on issues involved in ethical publication and affirm that this report is consistent with those guidelines.

Keywords

malformation; tractography; fMRI; epilepsy; dyslexia

Introduction

In many forms of epilepsy, aberrant neuronal connections are likely to be important in pathogenesis (Scharfman 2007). Unfortunately, our ability to probe these changes noninvasively in human patients has been limited. Periventricular nodular heterotopia (PNH), one of the most commonly encountered epileptic brain malformations (Sisodiya 2004), is an ideal substrate for the study of epileptogenic processes (Dubeau et al. 1995; Li et al. 1997; Aghakhani et al. 2005). Although PNH patients are not homogeneous, being characterized by different clinical and radiological features (Battaglia et al. 2006), the disorder is defined by gray matter nodules located along or extending from the walls of the lateral ventricles, and usually presents with the clinical triad of normal intelligence, epilepsy, and reading dysfluency (Chang et al. 2005; Chang et al. 2007; Battaglia & Granata 2008). Just under half of cases have mutations in the FLNA (filamin A) gene on Xq28 (Fox et al. 1998).

Intracranial electrode studies suggest that epileptogenesis in PNH may arise from circuits involving both heterotopic gray matter and overlying cortex (Kothare et al. 1998; Tassi et al. 2005). The fact that PNH patients do not develop seizures until young adulthood, on average, raises the possibility that aberrant circuit formation (or myelination of abnormal tracts) may take place over time. Conventional MRI shows normal-appearing cortex and white matter in PNH (Poussaint et al. 2000), although histological examination can reveal subtle cytoarchitectural changes (Kakita et al. 2002; Meroni et al. 2009). In some instances, myelinated fibers have been seen emanating from the heterotopia, although their destinations are unknown (Hannan et al. 1999).

The combined use of diffusion tensor imaging and functional connectivity MRI (fcMRI) offers a powerful means of characterizing the connectivity of the human brain *in vivo* (Eriksson et al. 2001; Di Martino et al. 2008; Greicius 2008; Guye et al. 2008; Whitfield-Gabrieli et al. 2009). We sought to use these methods in conjunction to map abnormal circuits in PNH that had not previously been identified, and to examine the relationship between these circuits and clinical factors in this population.

Methods

Subject recruitment and criteria

Subjects with PNH were recruited from a research database of patients with malformations of cortical development who had participated in prior studies, from a clinical database of epilepsy patients at our institution, and through research referrals from clinical neurologists. Patients with a neuroimaging-confirmed diagnosis of PNH based on the presence of at least two visible nodules of heterotopic gray matter adjacent to the lateral ventricle, each seen on more than one plane of sequence and on at least two consecutive images in one of those planes, were eligible to be enrolled. Those with prior brain surgery, inability to tolerate MRI, or a specific MRI contraindication as set forth in standard protocols of our institutions were excluded, as were pregnant women due to lack of definitive information on fetal safety in MRI.

Standard protocol approvals and patient consents

All subjects provided written informed consent in accordance with research protocols approved by the institutional review boards of Beth Israel Deaconess Medical Center and the Massachusetts Institute of Technology.

Image acquisition

Imaging was performed on a Siemens 3-Tesla Magnetom Trio Tim system using a commercial 12-channel matrix head coil (Siemens Medical Solutions, Erlangen, Germany) and tetrahedron-shaped foam pads to minimize head movement. Sagittal localizer scans were aligned to a multi-subject atlas to derive automatic slice prescription for consistent head position across subjects. High-resolution structural whole-brain images were acquired using a T1-weighted sequence with 128 slices per slab, a 256×256 matrix, a field of view (FOV) of 256 mm, a slice thickness of 1.33 mm with 0.63 mm interslice gap, repetition time (TR) of 2530 ms, inversion time (TI) of 1100 ms, echo time (TE) of 3.39 ms, and flip angle of 7 degrees. Diffusion-weighted imaging was performed using a spin-echo sequence with TR of 7980 ms, TE of 84 ms, FOV of 256 mm, voxel size of $2.0 \times 2.0 \times 2.0$ mm, b-value of 700, and 60 non-collinear directions. Resting-state functional image acquisition was performed while the subjects were asked to rest quietly (acquisition time 6.4 minutes), using an echo-planar sequence sensitive to blood oxygenation level-dependent (BOLD) contrast with TR of 6000 ms, TE of 30 ms, FOV of 256 mm, voxel size of $2.0 \times 2.0 \times 2.0$ mm, and flip angle of 90 degrees.

Structural connectivity analysis

Diffusion tensor analysis with fiber tractography was performed on the acquired image data using the Diffusion Toolkit software package (version 0.6.1), including the TrackVis fiber track visualization and analysis program (version 0.5.1; Wang et al. 2007). Diffusion-weighted images for each subject were realigned and coregistered to that subject's anatomical images without normalization due to concern about potentially inappropriate distortions in the presence of anomalous deep gray matter. The tractography method of fiber assignment by continuous tracking was employed (Mori et al. 1999), with propagation terminated for tract angle $> 70^\circ$ or if an automatically generated mask threshold was not reached.

Each discrete region of nodular heterotopia (either an individual nodule or an inseparable contiguous cluster of nodules) in each subject was identified and outlined manually (so as to avoid contamination with adjacent cerebrospinal fluid in the ventricles), slice by slice in the axial plane on T1-weighted anatomical images, as a region of interest (ROI) for TrackVis analysis in native space. (One subject [Subject 4] had two contiguous, inseparable nodules outlined as a single ROI.) Fiber tracks for which either terminus was located within the boundaries of the ROI were then visualized for every heterotopic region, and examined visually for anatomical plausibility. Fiber track density was calculated as tracks/voxel within the ROI.

Tractography results were displayed on T1-weighted anatomical images, and specific tract destinations were identified using a standard anatomical brain atlas. Each tract destination was categorized as belonging to ipsilateral cortex overlying the heterotopic region (within the same cerebral lobe), ipsilateral but nonoverlying cortex (different lobe), contralateral homologous cortex (same lobe), contralateral but nonhomologous cortex (different lobe), other heterotopia, or deep gray matter/cerebellum.

Functional connectivity analysis

fMRI analyses were performed on the functional image data acquired during the task-free resting state with an in-house software toolbox, using methods previously described (Fox et al. 2005; Whitfield-Gabrieli et al. 2009). Functional images were realigned and coregistered to anatomical images for each subject, without normalization. Images were segmented and BOLD signal was extracted. A band-pass frequency filter ($0.01 \text{ Hz} < f < 0.1 \text{ Hz}$) was applied, and Gaussian smoothing was performed (6 mm full width at half maximum). Several possible confounding sources of noise were identified and removed (Behzadi et al. 2007). For each subject, the same heterotopia ROIs described for structural connectivity analysis above were outlined in native space and served as seed regions for analysis. Color-coded functional connectivity maps were created for each seed ROI, showing correlations between the average BOLD signal time-series of the ROI and that of every voxel in the brain, subject to a voxel-wise statistical threshold of $p < 0.001$ and cluster thresholding with an intensity cutoff. Brain regions that were functionally connected to the seed heterotopia were then anatomically identified using a standard brain atlas. Correlated regions were categorized according to the same scheme described above for structural connectivity results.

Measures of clinical epilepsy and cognitive ability

The medical records of all subjects were reviewed to ascertain details of their clinical epilepsy, including estimated seizure frequency and age of seizure onset. In addition, all subjects were tested using a panel of behavioral reading tasks and reading-related measures specifically selected to assess reading fluency performance, based on past reports in this population (Chang et al. 2005; Chang et al. 2007). This included timed evaluation of word-level reading (Test of Word Reading Efficiency [TOWRE] - Single Word Efficiency [SWE]; Torgesen et al. 1999) and sublexical fluency skills (Comprehensive Test of Phonological Processing [CTOPP] - rapid automatized naming; Wagner et al. 1999), among other measures.

Statistical analysis

The degree of inter-method agreement between structural and functional connectivity findings with regard to aberrant connectivity was determined by calculation of the free-marginal kappa statistic across all heterotopic regions analyzed for all subjects (Siegel & Castellan 1988; Randolph 2008). Relationships among quantified structural and functional connectivity results and the clinical epilepsy and behavioral measures described above were analyzed using Student's t-test, the Mann-Whitney U test, and calculations of either Pearson's correlation coefficients for normally distributed data or Spearman's rank correlation for data that were not normally distributed (InStat 3.10, GraphPad Software, Inc., San Diego, CA). A significance threshold of $p < 0.05$ was applied for all analyses.

Results

Subject and heterotopia characteristics

Eleven subjects with PNH (seven female) were studied (Table 1). All were right-handed and the median age was 29 (range 19 to 76). All had a history of focal epilepsy with complex partial seizures, some with secondary generalization. The median age of seizure onset was 22 (range 8 to 75). Five subjects had medically well-controlled epilepsy, with no seizures in several years, while the remainder had seizure frequencies ranging from one every one and one half years to one every week. Confirming prior findings of reading dysfluency in this disorder (Chang et al. 2005; Chang et al. 2007), PNH subjects performed poorly on timed tests of word reading (mean TOWRE SWE scaled score 85, Z-score -1.0) and sublexical

rapid naming tasks (mean CTOPP rapid object naming scaled score 7.6, Z-score -1.6). Three subjects (1, 2, and 8) had previously been described in a prior cognitive and imaging study (Chang et al. 2007).

A total of 45 discrete regions of periventricular nodular heterotopia were identified and manually parcellated for analysis (mean 4.1 regions/subject, range 1–8; mean volume of heterotopic region 0.40 mL, range 0.02–1.35; Supporting Table). Heterotopia were distributed throughout the brains of the subjects and classified according to laterality (60% right-sided) as well as rostro-caudality (67% posterior).

Structural connectivity

Diffusion tensor tractography demonstrated that 31 of 45 (69%) heterotopic regions, including at least one in each subject except Subject 5, were at one terminus of at least one fiber track whose other end extended to a discrete region of overlying cortex (Supporting Table; Figure 1A). Heterotopic regions also showed structural connections to other ipsilateral but non-overlying regions of cortex (38%), regions of homologous contralateral cerebral cortex (49%), regions of nonhomologous contralateral cortex (13%), other heterotopic nodules (29%), and other subcortical and posterior fossa gray matter structures, such as the thalamus, basal ganglia, and cerebellum (42%; Figure 2A). The mean density of visualized fiber tracks with a terminus within a region of heterotopia, across all such regions, was 0.11 tracks/voxel (standard deviation [SD] 0.03).

Resting-state functional connectivity

With nodular heterotopia identified as seed ROIs for functional connectivity analysis using resting-state BOLD data, correlations between heterotopia and other voxels within the brain were determined. Forty-three of 45 (96%) regions of heterotopic gray matter, including at least one in each subject, showed functional connectivity to discrete regions of overlying cortex (Supporting Table; Figures 1B and 3). In 33% of these cases (31% of all heterotopia), overlying cortex was the brain region with highest correlation to the heterotopic seed region. Nodular heterotopia also demonstrated functional connectivity to ipsilateral non-overlying regions of cortex (42% of the time, with 18% of all heterotopia showing the highest correlation to these regions), homologous contralateral cortex (51%, with 13% most highly correlated; Figure 3D); contralateral but nonhomologous cortex (27%, with 9% most highly correlated); other heterotopia (51%; with 29% most highly correlated); and deep gray matter or cerebellum (13%; with 4% most highly correlated; Figure 2B). The mean peak functional correlation coefficient in the most highly correlated region, across all heterotopia, was 0.68 (SD 0.08).

For 69% of the heterotopic regions studied, diffusion tensor tractography and functional connectivity analyses were in agreement in demonstrating connectivity to discrete regions of overlying cortex (free-marginal kappa statistic 0.38, indicating moderate agreement beyond chance; Supporting Table). There was no significant relationship between the density of fiber tracks within each heterotopic region and the degree of peak functional correlation, nor between either of these measures and heterotopic region volume.

Clinical epilepsy and cognitive analyses

The single highest peak correlation coefficient within a brain region showing functional connectivity to any heterotopic nodule was recorded as a quantified measure of the degree of abnormal connectivity in each individual subject. This measure was significantly higher in the two subjects who had had epilepsy for more than three decades than in the remainder of the subjects, who all had epilepsy for far shorter periods of time (mean peak correlation 0.82 vs. 0.74, $p=0.036$ by Mann-Whitney U test). The degree of abnormal connectivity was not

correlated with age of epilepsy onset, seizure frequency, or number of days since last seizure, nor with scores on timed measures of word-level reading or sublexical rapid naming.

Discussion

Here we demonstrate that regions of nodular heterotopia in a developmental brain malformation show connectivity to other regions of gray matter in the brain, most prominently to discrete regions of cerebral cortex that immediately overlie the heterotopia themselves. Our use of diffusion tensor tractography and resting-state functional connectivity imaging in conjunction allows us not just to identify white matter fiber tracks mediating structural connectivity between heterotopia and other brain regions, but also to demonstrate that these structurally connected areas are highly functionally correlated as well.

Our work represents the first systematic demonstration of such connectivity in gray matter heterotopia, but is consistent with existent literature suggesting that abnormal circuits may develop between heterotopic gray matter and normal gray matter in various brain malformations. For example, histological studies of postmortem human brain tissue in PNH have demonstrated myelinated fibers coming from the nodules (Hannan et al. 1999), but the scarcity of tissue and limitations of tracer techniques have not allowed for more definitive studies. Intracranial recordings have shown simultaneous epileptiform EEG discharges from heterotopia and cortex, suggesting functional connections (Kothare et al. 1998; Tassi et al. 2005), but these have required invasive electrode implantation, usually in patients undergoing evaluation for epilepsy surgery. Similarly, case reports of task-based and EEG-linked functional MRI experiments have identified simultaneous activation within heterotopia and segments of overlying cortex (Pinard et al. 2000; Janszky et al. 2003; Archer et al. 2010), but the use of such methods must typically be individualized for each subject and often requires *a priori* assumptions about heterotopia functionality, unlike our present methods, which were applied systematically to nodules in different locations in different subjects.

We find that structural connectivity and functional connectivity results are in reasonable agreement, although functional connectivity between heterotopia and other gray matter regions was seen more commonly and in more locations (49.6% of functional connectivity instances did not have a diffusion tractography counterpart), and there was no simple relationship between fiber tract density and degree of functional correlation. These findings are likely explained by the known ability of functional connectivity methods to demonstrate correlations between regions that may be connected across multiple synapses, are anatomically distant from each other, and/or show correlation because of common connectivity to a third area without being directly connected themselves (Guye et al. 2008). Commonly used diffusion tractography algorithms, including the one employed here, impose boundaries on tract generation to enforce biological plausibility among the visualized results.

Genetic, molecular, and immunohistochemical evidence suggests that the neurons in nodular heterotopia are of normal morphology and were destined to migrate toward the developing cortical plate, but failed to do so (Fox et al. 1998; Ferland et al. 2009). One might expect then that these heterotopic neurons could form connections with cortical neurons in their intended destination (the overlying regions of cortex to which they would have radially migrated), as well as with other regions of ipsilateral and contralateral cortex, through tracts analogous to the association and commissural fibers seen projecting from normal cortical neurons. Indeed, we found that overlying cortex and homologous contralateral cortex were

the most frequent gray matter segments to which nodular heterotopia showed structural and functional connectivity. Interestingly, we identified a few cases in which diffusion tensor tracts extended from heterotopia to the cerebellar hemispheres (Figure 2), although no direct monosynaptic projections from cerebral cortex to cerebellar cortex normally exist; the significance of this finding is unclear but it may need to be confirmed in larger samples.

Our connectivity results in PNH, a highly epileptogenic brain malformation, taken together with the existing evidence of aberrant fiber sprouting as a critical element in other models of epilepsy (Dudek & Sutula 2007; Rakhade & Jensen 2009), support the speculation that the abnormal structural and functional relationships we demonstrate here may be a causal factor in the generation of an epileptogenic state in this disorder. Consistent with this notion is the relationship between epilepsy duration and peak degree of functional connectivity, suggesting that the strength of the abnormal circuitry may increase over time. Indeed, epileptogenesis is not a process that stops upon the appearance of the first or second spontaneous seizure but is presumed to continue even as further clinical seizures occur (Scharfman 2007).

Several possible mechanisms may underlie the development of a tendency toward seizures in the presence of aberrant fiber sprouting, as suggested by other well-validated models of epilepsy; for example, there may be an intrinsic hyperexcitability of the cortical partner regions of heterotopia due to aberrant feedback loops without appropriate inhibitory constraints (Dudek & Sutula 2007; Scharfman 2007; Rakhade & Jensen 2009). The changes in functional circuitry accompanying some forms of epilepsy may be complex, however; there is evidence, for example, that basal connectivity in mesial temporal lobe epilepsy may actually be decreased ipsilaterally to the focus but increased contralaterally (Bettus et al. 2009), although EEG-based and BOLD-based connectivity measures may give discordant results (Bettus et al. 2011).

There are several discrete limitations to our work. Diffusion tensor imaging (DTI) cannot distinguish afferent and efferent projections, and since our voxels are 2 mm in each dimension, true axonal tractography at a submillimeter level cannot be achieved. In addition, DTI can only reveal the dominant orientation of fiber tracts within any given voxel and is unable to resolve mixtures of crossing fiber populations (Mori et al. 2005). Resting-state fMRI relies on correlations in a very low-frequency range ($< \sim 0.1$ Hz) so possible correlations of significance at higher frequencies would not be captured using our method (Allen et al. 2005; Fair et al. 2009). There is also no way to substantiate the nature of the true “resting state”, since it is not possible to determine exactly what subjects are doing during this time, but reproducible findings using fMRI have been obtained across multiple studies and subject populations to date. We did not employ simultaneous EEG recording during connectivity image acquisition, which could have provided additional information on the relationship between our findings and neurophysiologic activity. Others have examined functional connectivity linked to interictal or ictal epileptiform activity in cortical malformations (Tyvaert et al. 2008; Archer et al. 2010); our results, obtained during the resting state, are not EEG-linked but are unlikely to be contaminated by unexpected epileptiform activity given the relative infrequency of clinical seizures and very low baseline spike frequency in most of our subjects. Finally, because only one of our subjects had a documented FLNA mutation, we were unable to explore the effect, of any, of genetics directly on connectivity.

Despite these limitations, our findings have important implications for our understanding of epileptogenesis in PNH and related developmental brain disorders. Data from our previous study demonstrated that disruptions in cortico-cortical tracts are likely to serve as the structural basis for the reading disability in this population (Chang et al. 2007).

Incorporating these prior data with the current findings, we propose a model in which connectivity defects may be responsible for both key aspects of the neurological phenotype in PNH (Figure 4). We speculate that loss of cortico-cortical connectivity in regions necessary for fluent reading may be responsible for the reading phenotype in this disorder, while the presence of aberrant connectivity between heterotopic nodules and discrete cortical partner regions may underlie the epileptogenic state.

A number of open issues require future investigation. It would be important to assess using physiological methods whether aberrantly connected regions of gray matter contain neurons that are indeed intrinsically hyperexcitable as a result of their structural and functional changes, as noted above. Since it takes 22 years on average for seizures to develop in PNH, longitudinal imaging studies in childhood might allow us to establish the time course of the appearance and development of the abnormal connectivity shown here. Larger numbers of subjects would also allow for a more nuanced analysis of various anatomical subtypes of PNH, which was not possible here due to small sample size and heterotopia heterogeneity. The evidence to date, however, strongly suggests that an optimal understanding of the neurological pathophysiology of “gray matter heterotopia” will come as much from an appreciation of how these misplaced clusters of neurons are connected, as from the clusters themselves.

Supplementary Material

Refer to Web version on PubMed Central for supplementary material.

Acknowledgments

We thank our subjects and their families, without whom this study could not have been performed. Josef Parvizi provided additional clinical information. Mollie E. Barnard assisted with structural MRI analysis and manuscript editing. Bernard S. Chang was supported by the National Institutes of Health / National Institute of Neurological Disorders and Stroke (R01 NS073601, K23 NS049159), the Epilepsy Foundation, and the William F. Milton Fund of Harvard University.

References

- Aghakhani Y, Kinay D, Gotman J, Soualmi L, Andermann F, Olivier A, Dubeau F. The role of periventricular nodular heterotopia in epileptogenesis. *Brain*. 2005; 128:641–651. [PubMed: 15659421]
- Allen G, McColl R, Barnard H, Ringe WK, Fleckenstein J, Cullum CM. Magnetic resonance imaging of cerebellar-prefrontal and cerebellar-parietal functional connectivity. *NeuroImage*. 2005; 28:39–48. [PubMed: 16023375]
- Archer JS, Abbott DF, Masterton RA, Palmer SM, Jackson GD. Functional MRI interactions between dysplastic nodules and overlying cortex in periventricular nodular heterotopia. *Epilepsy Behav*. 2010; 19:631–634. [PubMed: 21030316]
- Battaglia G, Chiapparini L, Franceschetti S, Freri E, Tassi L, Bassanini S, Villani F, Spreafico R, D’Incerti L, Granata T. Periventricular nodular heterotopia: classification, epileptic history, and genesis of epileptic discharges. *Epilepsia*. 2006; 47:86–97. [PubMed: 16417536]
- Battaglia, G.; Granata, T. Periventricular nodular heterotopia. In: Sarnat, HB.; Curatolo, P., editors. *Handbook of Clinical Neurology*, Vol. 87 (3rd series), Malformations of the Nervous System. Amsterdam: Elsevier; 2008. p. 177-190.
- Behzadi Y, Restom K, Liu J, Liu TT. A component based noise correction method (CompCor) for BOLD and perfusion based fMRI. *Neuroimage*. 2007; 37:90–101. [PubMed: 17560126]
- Bettus G, Guedj E, Joyeux F, Confort-Gouny S, Soulier E, Laguitton V, Cozzone PJ, Chauvel P, Ranjeva JP, Bartolomei F, Guye M. Decreased basal fMRI functional connectivity in epileptogenic networks and contralateral compensatory mechanisms. *Hum Brain Mapp*. 2009; 30:1580–1591. [PubMed: 18661506]

- Bettus G, Ranjeva JP, Wendling F, Benar CG, Confort-Gouny S, Regis J, Chauvel P, Cozzone PJ, Lemieux L, Bartolomei F, Guye M. Interictal functional connectivity of human epileptic networks assessed by intracerebral EEG and BOLD signal fluctuations. *PLoS One*. 2011; 6:e20071. [PubMed: 21625517]
- Chang BS, Katzir T, Liu T, Corriveau K, Barzillai M, Apse KA, Bodell A, Hackney D, Alsop D, Wong ST, Walsh CA. A structural basis for reading fluency: white matter defects in a genetic brain malformation. *Neurology*. 2007; 69:2146–2154. [PubMed: 18056578]
- Chang BS, Ly J, Appignani B, Bodell A, Apse KA, Ravenscroft RS, Sheen VL, Doherty MJ, Hackney DB, O'Connor M, Galaburda AM, Walsh CA. Reading impairment in the neuronal migration disorder of periventricular nodular heterotopia. *Neurology*. 2005; 64:799–803. [PubMed: 15753412]
- Di Martino A, Scheres A, Margulies DS, Kelly AM, Uddin LQ, Shehzad Z, Biswal B, Walters JR, Castellanos FX, Milham MP. Functional connectivity of human striatum: a resting state fMRI study. *Cereb Cortex*. 2008; 18:2735–2747. [PubMed: 18400794]
- Dubeau F, Tampieri D, Lee N, Andermann E, Carpenter S, Leblanc R, Olivier A, Radtke R, Villemure JG, Andermann F. Periventricular and subcortical nodular heterotopia: A study of 33 patients. *Brain*. 1995; 118:1273–1287. [PubMed: 7496786]
- Dudek FE, Sutula TP. Epileptogenesis in the dentate gyrus: a critical perspective. *Prog Brain Res*. 2007; 163:755–773. [PubMed: 17765749]
- Eriksson SH, Rugg-Gunn FJ, Symms MR, Barker GJ, Duncan JS. Diffusion tensor imaging in patients with epilepsy and malformations of cortical development. *Brain*. 2001; 124:617–626. [PubMed: 11222460]
- Fair DA, Cohen AL, Power JD, Dosenbach NU, Church JA, Miezin FM, Schlaggar BL, Petersen SE. Functional brain networks develop from a “local to distributed” organization. *PLoS Comput Biol*. 2009; 5(5) e1000381.
- Ferland RJ, Batiz LF, Neal J, Lian G, Bundock E, Lu J, Hsiao YC, Diamond R, Mei D, Banham AH, Brown PJ, Vanderburg CR, Joseph J, Hecht JL, Folkerth R, Guerrini R, Walsh CA, Rodriguez EM, Sheen VL. Disruption of neural progenitors along the ventricular and subventricular zones in periventricular heterotopia. *Hum Mol Genet*. 2009; 18:497–516. [PubMed: 18996916]
- Fox JW, Lamperti ED, Ekioylu YZ, Hong SE, Feng Y, Graham DA, Scheffer IE, Dobyns WB, Hirsch BA, Radtke RA, Berkovic SF, Huttenlocher PR, Walsh CA. Mutations in filamin 1 prevent migration of cerebral cortical neurons in human periventricular heterotopia. *Neuron*. 1998; 21:1315–1325. [PubMed: 9883725]
- Fox MD, Snyder AZ, Vincent JL, Corbetta M, Van Essen DC, Raichle ME. The human brain is intrinsically organized into dynamic, anticorrelated functional networks. *Proc Natl Acad Sci USA*. 2005; 102:9673–9678. [PubMed: 15976020]
- Greicius M. Resting-state functional connectivity in neuropsychiatric disorders. *Curr Opin Neurol*. 2008; 21:424–430. [PubMed: 18607202]
- Guye M, Bartolomei F, Ranjeva J-P. Imaging structural and functional connectivity: towards a unified definition of human brain organization? *Curr Opin Neurol*. 2008; 21:393–403. [PubMed: 18607198]
- Hannan AJ, Servotte S, Katsnelson A, Sisodiya S, Blakemore C, Squier M, Molnár Z. Characterization of nodular neuronal heterotopia in children. *Brain*. 1999; 122:219–238. [PubMed: 10071051]
- Janzky J, Ebner A, Kruse B, Mertens M, Jokeit H, Seitz RJ, Witte OW, Tuxhorn I, Woermann FG. Functional organization of the brain with malformations of cortical development. *Ann Neurol*. 2003; 53:759–767. [PubMed: 12783422]
- Kakita A, Hayashi S, Moro F, Guerrini R, Ozawa T, Ono K, Kameyama S, Walsh CA, Takahashi H. Bilateral periventricular nodular heterotopia due to *filamin 1* gene mutation: widespread glomeruloid microvascular anomaly and dysplastic cytoarchitecture in the cerebral cortex. *Acta Neuropathol*. 2002; 104:649–657. [PubMed: 12410386]
- Kothare SV, VanLandingham K, Armon C, Luther JS, Friedman A, Radtke RA. Seizure onset from periventricular nodular heterotopias: depth-electrode study. *Neurology*. 1998; 51:1723–1727. [PubMed: 9855532]

- Li LM, Dubeau F, Andermann F, Fish DR, Watson C, Cascino GD, Berkovic SF, Moran N, Duncan JS, Olivier A, Leblanc R, Harkness W. Periventricular nodular heterotopia and intractable temporal lobe epilepsy: poor outcome after temporal lobe resection. *Ann Neurol*. 1997; 41:662–668. [PubMed: 9153529]
- Meroni A, Galli C, Bramerio M, Tassi L, Colombo N, Cossu M, Lo Russo G, Garbelli R, Spreafico R. Nodular heterotopia: a neuropathological study of 24 patients undergoing surgery for drug-resistant epilepsy. *Epilepsia*. 2009; 50:116–124. [PubMed: 18637832]
- Mori S, Crain BJ, Chacko VP, van Zijl PC. Three-dimensional tracking of axonal projections in the brain by magnetic resonance imaging. *Ann Neurol*. 1999; 45:265–269. [PubMed: 9989633]
- Mori, S.; Wakana, S.; Nagae-Poetscher, LM.; van Zijl, PCM. MRI atlas of human white matter. Amsterdam: Elsevier Inc.; 2005. Limitations of DTI-based reconstruction; p. 9-10.
- Pinard JM, Feydy A, Carlier R, Perez N, Pierot L, Burnod Y. Functional MRI in double cortex: functionality of heterotopia. *Neurology*. 2000; 54:1531–1533. [PubMed: 10751274]
- Poussaint TY, Fox JW, Dobyns WB, Radtke R, Scheffer IE, Berkovic SF, Barnes PD, Huttenlocher PR, Walsh CA. Periventricular nodular heterotopia in patients with filamin-1 gene mutations: neuroimaging findings. *Pediatr Radiol*. 2000; 30:748–755. [PubMed: 11100490]
- Rakhade SN, Jensen FE. Epileptogenesis in the immature brain: emerging mechanisms. *Nat Rev Neurol*. 2009; 5:380–391. [PubMed: 19578345]
- Randolph JJ. Online Kappa Calculator. 2008 from <http://justus.randolph.name/kappa>.
- Scharfman HE. The neurobiology of epilepsy. *Curr Neur Neurosci Rep*. 2007; 7:348–354.
- Siegel, S.; Castellan, NJ. Nonparametric statistics for the social sciences. 2nd ed.. New York: McGraw-Hill; 1988.
- Sisodiya SM. Malformations of cortical development: burdens and insights from important causes of human epilepsy. *Lancet Neurol*. 2004;29–38. [PubMed: 14693109]
- Tassi L, Colombo N, Cossu M, Mai R, Francoine S, Lo Russo G, Galli C, Bramerio M, Battaglia G, Garbelli R, Meroni A, Spreafico R. Electroclinical, MRI and neuropathological study of 10 patients with nodular heterotopia, with surgical outcomes. *Brain*. 2005; 128:321–337. [PubMed: 15618282]
- Torgesen, JK.; Wagner, R.; Rashotte, C. Test of Word Reading Efficiency (TOWRE). Austin: Pro-Ed; 1999.
- Tyvaert L, Hawco C, Kobayashi E, LeVan P, Dubeau F, Gotman J. Different structures involved during ictal and interictal epileptic activity in malformations of cortical development: an EEG-fMRI study. *Brain*. 2008; 131:2042–2060. [PubMed: 18669486]
- Wagner, R.; Torgesen, JK.; Rashotte, C. Comprehensive Test of Phonological Processing (CTOPP). Austin: Pro-Ed; 1999.
- Wang R, Benner T, Sorensen AG, Wedeen VJ. Diffusion toolkit: a software package for diffusion imaging data processing and tractography. *Proc Intl Soc Mag Reson Med*. 2007; 15:3720.
- Whitfield-Gabrieli S, Thermenos HW, Milanovic S, Tsuang MT, Faraone SV, McCarley RW, Shenton ME, Green AI, Nieto-Castanon A, LaViolette P, Wojcik J, Gabrieli JD, Seidman LJ. Hyperactivity and hyperconnectivity of the default network in schizophrenia and in first-degree relatives of persons with schizophrenia. *Proc Natl Acad Sci USA*. 2009; 106:1279–1284. [PubMed: 19164577]

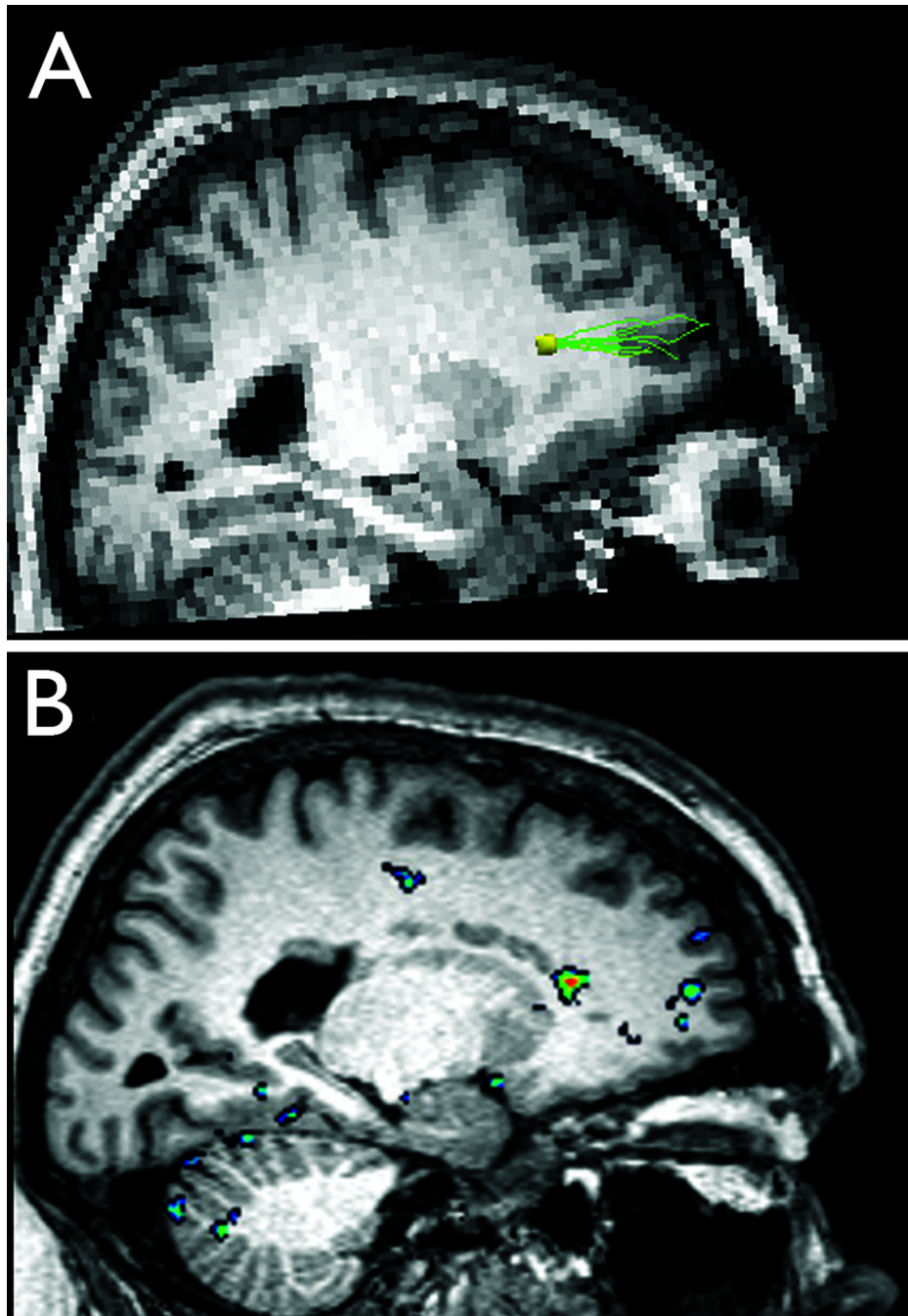


Figure 1. Structural and functional connectivity of periventricular heterotopia to overlying cerebral cortex

Diffusion tensor tractography results co-registered on T1-weighted sagittal anatomical MR image (A) show fiber tracks (green) extending from a left frontal periventricular nodule of heterotopic gray matter (yellow; heterotopia 2–6 in Supporting Table) anteriorly to a discrete region of overlying cerebral cortex. Resting-state functional connectivity analyses (B) show correlation between the same heterotopic nodule (bright orange center) and the same region of overlying cortex (green center; peak correlation coefficient 0.52).

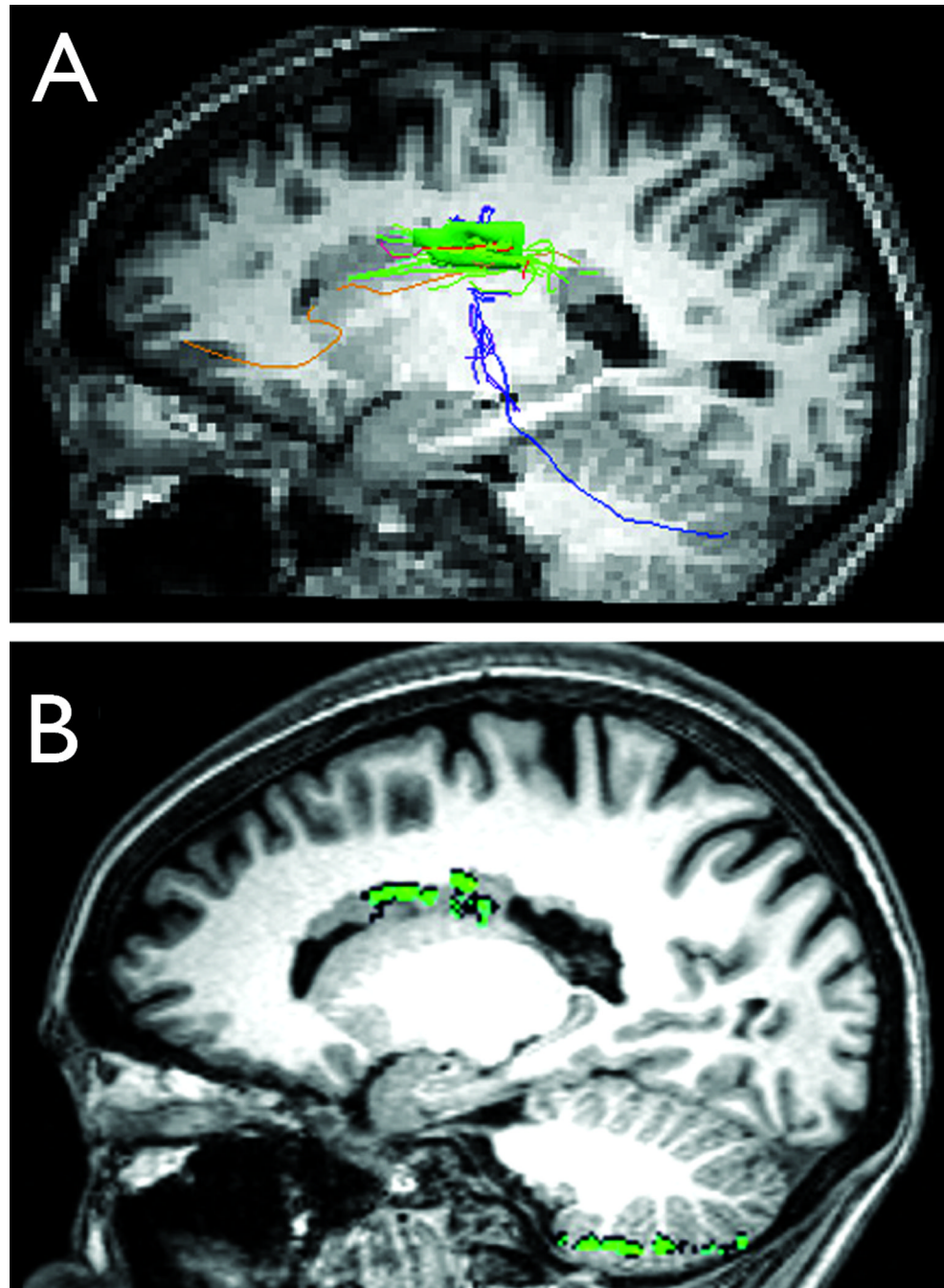


Figure 2. Structural and functional connectivity of periventricular heterotopia to cerebellum Diffusion tensor tractography results co-registered on T1-weighted sagittal anatomical MR image (**A**) show fiber tracks (blue) extending from a large, confluent region of right periventricular heterotopia (green; heterotopia 5-2 in Supporting Table) to the ipsilateral cerebellar hemisphere. Resting-state functional connectivity analyses (**B**) show correlation between the same heterotopia and the ipsilateral cerebellar gray matter (green areas; peak correlation coefficient 0.59).

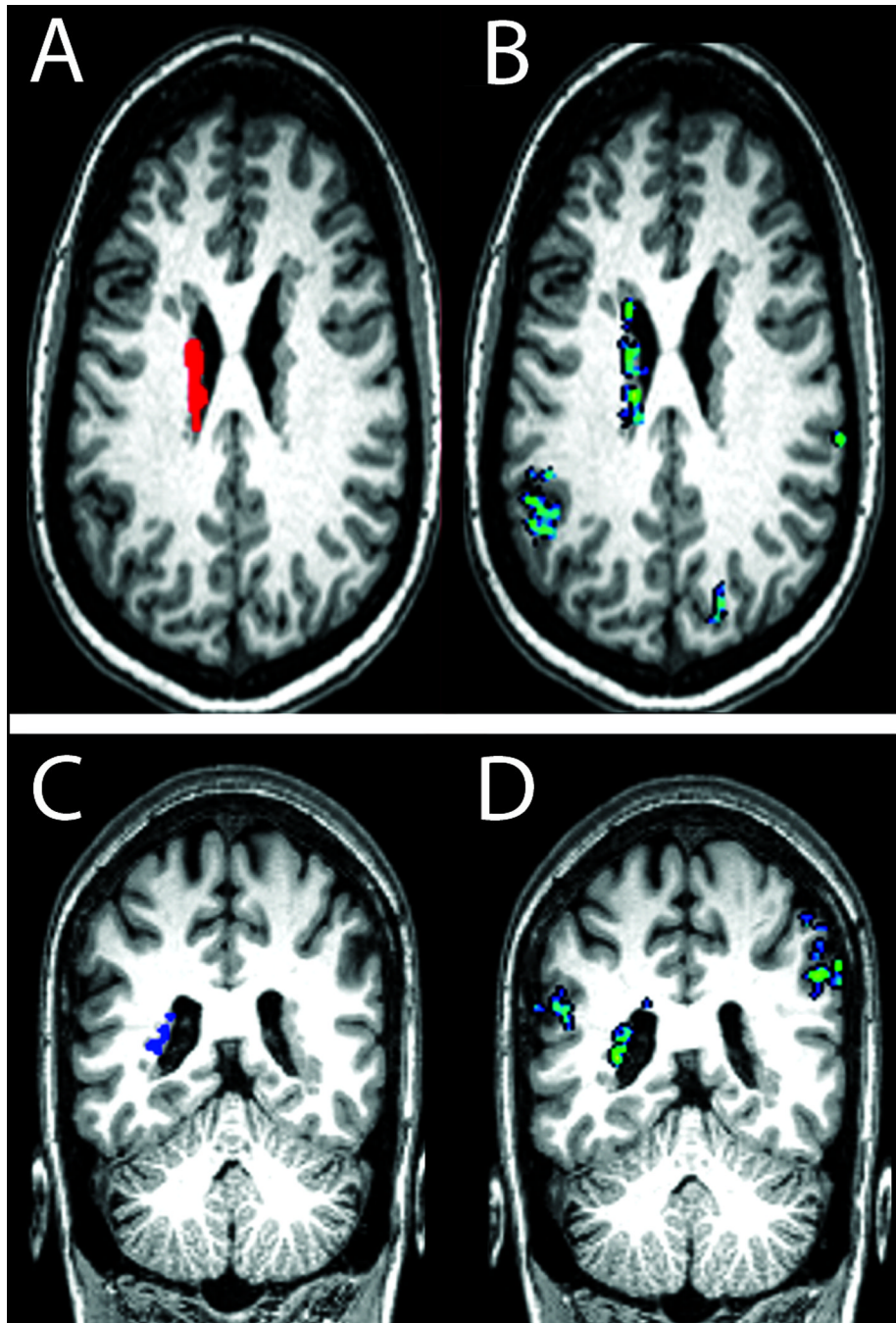


Figure 3. Functional connectivity of periventricular heterotopia to ipsilateral and contralateral cortical regions

With an extensive left-sided region of heterotopia identified in one subject (top) as a seed region for resting-state functional connectivity analysis (red in **A**; heterotopia 1–6 in Supporting Table), a highly functionally correlated region of overlying cortex was seen within the left supramarginal gyrus (blue/green in **B**; peak correlation coefficient 0.61). In another subject (bottom), a left posterior region of heterotopia was identified as a seed region for connectivity analysis (blue in **C**; heterotopia 8-3 in Supporting Table); highly functionally correlated regions were seen in the left superior temporal gyrus and right

supramarginal gyrus (blue-green areas in **D**; peak correlation coefficients 0.53 and 0.56, respectively).

Reading dysfluency

Disrupted cortico-cortical connections

Aberrant cortico-heterotopic connections

Epilepsy

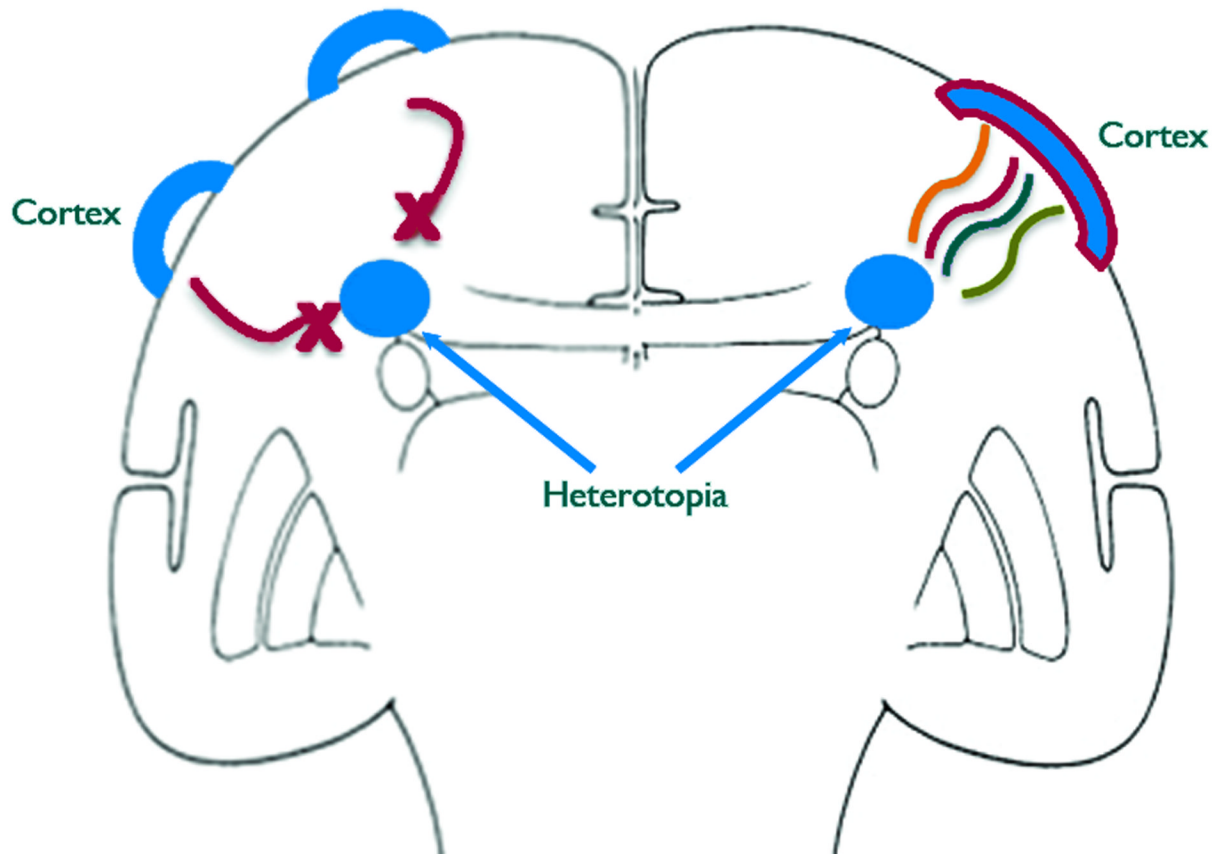


Figure 4. A connectivity model of neurological dysfunction in gray matter heterotopia

In this model, based on data from this paper and prior work (Chang et al. 2007), the reading dysfluency seen in periventricular nodular heterotopia is related to disruptions in cortico-cortical tracts that normally connect regions of brain important for reading fluency, while epileptogenesis is related to aberrant connections between heterotopic gray matter and overlying cortex.

Table 1

Characteristics of periventricular nodular heterotopia subjects.

Subject	Cognitive Profile			Clinical Epilepsy			Genetics		Heterotopia Characteristics	
	Age (yrs)/ Handed/Sex	VIQ/PIQ/ FSIQ	TOWRE SWE scaled	Age at onset (yrs)	Seizure type and frequency	EEG results	FLNA mutation	Number and laterality	Location	
1	32/R/F	104/100/103	83	24	Well-controlled CPS	Normal routine EEG	No	~8R/~5L	Diffuse	
2	42/R/M	127/111/122	113	8	1 CPS every 2 wks	Bifrontal/bitemporal ictal onset; no interictal discharges	No	3R/3L	Trigones, frontal horns	
3	76/R/M	100/114/108	75	75	None in 11 mos (CPS)	Not performed	Not tested	3R	Posterior body/trigone	
4	27/R/F	109/119/116	84	22	Well-controlled CPS	R frontotemporal slowing; no interictal discharges	Not tested	2R	Trigone	
5	27/R/F	NA	84	25	1 CPS every 1½ yrs	Normal routine EEG	No	~7R	Diffuse	
6	29/R/F	129/95/112	109	23	Well-controlled CPS	Normal routine EEG	Splice site mutation	~4R/~5L	Trigone, frontal horns	
7	21/R/M	94/89/90	77	17	1 CPS every yr	Normal routine EEG	No	1R/~5L	Posterior bodies, trigone	
8	40/R/F	106/98/103	91	23	Well-controlled CPS	Occasional R temporal spikes (none on 24-hour EEG)	No	2R/~4L	Trigones	
9	61/R/F	VIQ 70/PIQ 74	68	13	Well-controlled CPS	Broad L hemisphere ictal onset; L temporal interictal discharges	No	6R/6L	Diffuse	
10	21/R/M	57/83/68	59	8	1 CPS every 2 mos	R frontal ictal onset; R frontal interictal discharges	Not tested	3R	Trigone	
11	19/R/F	117/106/113	92	14	1 CPS every wk	Normal routine EEG	No	2R/~3L	Temporal horns, trigone	

Abbreviations: yrs = years; R = right; L = left; F = female; M = male; VIQ = verbal intelligence quotient; PIQ = performance intelligence quotient; FSIQ = full-scale intelligence quotient; NA = not available; TOWRE SWE = Test of Word Reading Efficiency Sight Word Efficiency standard score; CPS = complex partial seizures; wks = weeks; mos = months; FLNA = human *FLNA* gene; ~ = number is approximate due to confluent, inseparable nodules.